Journal of Magnetism and Magnetic Materials 401 (2016) 949–955

Contents lists available at ScienceDirect

Journal of Magnetism and Magnetic Materials

journal homepage: www.elsevier.com/locate/jmmm

γ-Fe_2O_3 magnetic nanoparticle functionalized with carboxylated multi walled carbon nanotube: Synthesis, characterization, analytical and biomedical application

Ersin Kılınç

Health Services, Vocational High School, Medical Marketing and Promotion Program, Mardin Artuklu University, 47200 Mardin, Turkey

ARTICLE INFO

Article history:
Received 19 February 2014
Received in revised form
27 October 2015
Accepted 1 November 2015
Available online 9 November 2015

Keywords:
Magnetic nanomaterials
Chemical synthesis
Magnetic properties
Controlled drug release
Characterization

ABSTRACT

In recent years, magnetic nanoparticles attained special interest in nanobiotechnology and nanomedicine due to their uniqe properties and biocompatibilities. From this perspective, hybride nanostructure composed from γ-Fe_2O_3 magnetic nanoparticle and carboxylated multi walled carbon nanotube was synthesized and characterized by FT-IR, VSM, SEM, HR-TEM and ICP-OES. Microscopy images showed that magnetic nanoparticles were nearly spherical structure that arranged on the axis of carboxylated MWCNT. Particle size was found lower than 10 nm. VSM results showed that the obtained magnetic nanoparticles presented superparamagnetic properties at room temperature. The magnetic saturation value was determined as 35.2 emu/g. It was used for the adsorption and controlled release of harmane, a potent tremor-producing neurotoxin. Maximum adsorption capacity was calculated as 151.5 mg/g from Langmuir isotherm. Concentration of harmane was determined by HPLC with fluorescence detection. The antimicrobial activity of synthesized magnetic nanoparticle was investigated against gram-negative and gram-positive bacteria. However, no activity was observed.

1. Introduction

Synthesis, characterization, analytical and biomedical applications of magnetic nanoparticles are of growing interest in nanoscience that significant efforts have been devoted to develop nanometer sized products for nanobiotechnology and nanomedicine. Materials such as polymeric nanomaterials, fullerene [1], single walled carbon nanotube (SWCNT), multi walled carbon nanotube (MWCNT) [2], quantum dots (QD) [3], magnetic nanoparticles (MNPs) [4] attained great interest in a wide range of applications. Special interest has been focused to MNPs in biomedical applications due to their biocompatibilities [5,6]. These include bioanalytical sensor [7], drug carrier [8], enzyme support material [9], magnetic resonance imaging (MRI) enhancement [10], targeted drug delivery [11], cancer diognasis and therapy [12].

Superparamagnetic iron oxide nanoparticles (SPIONs) have emerged as one of the most widely used materials. Among them, Fe_3O_4 (magnetite), rhombohedral α-Fe_2O_3 (hematite) and cubic γ-Fe_2O_3 (maghemite), ferrofluids, Fe–Ni are common [13–15]. γ-Fe_2O_3 is known as the most commonly used magnetic nanoparticle due to its availability, stability, low environmental impact and high magnetic susceptibility [16]. A protective shell for core magnetic structure is required to provide the long-term usability and reduce the agglomeration [15]. Core–shell structure is also needed to increase the stability and decrease the cytotoxicity of MNPs [17]. Coating would allow designing and functionalizing the MNPs to targeted applications. In addition, superparamagnetic properties of MNPs with core–shell structure should be protected to allow magnetic hyperthermia in case of *in vivo* applications [18]. Functionalized SPIONs are very promising for different applications. Surfactant and polymer coating, precious-metal coating, silica coating, carbon coating include SWCNT and MWCNT are commonly employed for protecting the magnetic core [19]. In this paper, special interest was focused on the functionalization of SPIONs by MWCNTs due to their importance and relevancy. MWCNT discovered by Iijima [20] was also found important applications in drug delivery, cancer therapy etc. [21,22]. It was highlighted that MWCNT was accepted as potential biomedical material due to its structure. However, functionalization is also required for biocompatibility and solubility [23].

Abbreviations: FD, Fluorescence dedector; FT-IR, Fourier transform infrared spectroscopy; HPLC, High performance liquid chromatography; HR-TEM, High-resolution transmittance electron microscopy; ICP-OES, Inductively coupled plasma optical emission spectrometry; MNPs, Magnetic nanoparticles; MRI, Magnetic resonance imaging; MWCNT, Multi walled carbon nanotube; NA, Nutrient agar; NB, Nutrient broth; QD, Quantum dot; SEM, Scanning electron microscopy; SPIONs, Superparamagnetic iron oxide nanoparticles; SWCNT, Single walled carbon nanotube; VSM, Vibrating sample magnetometer; XRD, X-ray diffractometer

E-mail address: kilincersin@gmail.com

http://dx.doi.org/10.1016/j.jmmm.2015.11.003
0304-8853/

Hydrophilic multi-walled carbon nanotubes decorated with Fe_3O_4 MNPs was used as lymphatic targeted drug delivery vehicles [24]. MWCNT core-Fe_3O_4 shell structure was synthesized; characterised and biomedical applications were investigated. Shan et al. reported that it had antimicrobial activities to bacterial cells (Escherichia coli) [25]. MWCNT-Fe_3O_4 prepared by solvothermal process was also used in magnetic targeted drug delivery system. Adsorption and release of epirubicin hydrochloride (anticancer drug) by MWCNT-Fe_3O_4 were investigated with details [26]. Fe_3O_4 nanoparticle enclosure hydroxylated MWCNT was used for the preconcentrations of mesaconitine, aconitine, hypaconitine in human serum through the magnetic extraction [27]. Song et al. synthesized the MWCNTs/β-FeOOH nanocomposite that showed a high adsorption capacity versus Congo red [28]. Amino and carboxyl modified MWCNT bounded to C18 and silica coated Fe_3O_4 MNPs were used to magnetic solid phase extraction of estrogens in milk samples [29]. Nanocomposite films prepared from MWCNT and Fe_3O_4 were used as dopant materials to enhance the electrical conductivity of chitosan nanocomposite films [30]. Deng et al. synthesized the Fe_3O_4-MWCNTs hybrid material by a solvothermal process using acid treated MWCNTs and iron acetylacetonate in a mixed solution of ethylene glycol and ultrapure water and it was used as Fenton-like catalyst to decompose acid orange II and displayed higher activity than nanometer-size Fe_3O_4 [31].

Harmane (1-methyl-9H-pyrido[3,4-*b*]indole) is known as one of the most potent tremor producing β-carboline alkaloids. Louis et al. reported that essential tremor was neurological disease that affected older people [32,33]. It is also noted that harmane is produced endogenously however it is also determined in foods and beverages [33,34].

In this research paper, carboxyl functionalized MWCNT-γ-Fe_2O_3 MNPs was synthesized and characterized by FT-IR, VSM, SEM, HR-TEM and ICP-OES. Analytical and bioanalytical applications of MWCNT-γ-Fe_2O_3 MNPs were investigated through the antimicrobial activity and adsorption/release of harmane. Harmane concentration was determined by HPLC with fluorescence detection.

2. Materials and methods

2.1. Reagents and standarts

Multiwalled carbon nanotube (o.d. 10–15 nm, i.d. 2–6 nm, length 0.1–10 μm), toluene, NH_4OH and harmane (> 98%) were supplied from Sigma-Aldrich. $FeCl_3 \cdot 6H_2O$, $FeCl_2$, KH_2PO_4 and K_2HPO_4 were bought from Merck and Fluka. All chemicals were analytical reagent-grade. Doubly distilled water was used through the experiments.

The antimicrobial activities of the γ-Fe_2O_3, cMWCNT, and cMWCNT-γ-Fe_2O_3 were tested against five different microorganisms. The gram-negative bacteria, namely *E. coli* ATCC 25922, *Pseudomonas aeruginosa* ATCC 27853, the gram positive bacteria namely *Staphylococcus aureus* ATCC 25923, *Streptococcus pyogenes* ATCC19615 and *Candida albicans* ATCC10231 were used for the study. Microorganisms were purchased from Refik Saydam Sanitation Center, Turkey.

2.2. Instrumentation

Concentrations of Fe in synthesized cMWCNT-γ-Fe_2O_3 magnetic nanoparticle and pristine MWCNT were determined by ICP-OES (Perkin Elmer, Optima 2100 DV) at the wavelength of 238.204 nm after acidic digestion. Instrumental conditions were given in our previous manuscript [35]. Infrared spectra of MNPs and cMWCNT were recorded on KBr pellet in the ranges 4000–400 cm^{-1} by FT-IR (Mattson Model 1000). The Model P525 Vibrating Sample Magnetometer (VSM) measurement system (Quantum Design) for the Physical Property Measurement System (PPMS) was used at 27 °C. SEM and HR-TEM images were recorded using a LEO-Evo 40 XVP scanning electron microscope and Jeol JEM 2100F HRTEM instrument working at 200 kV with a probe size under 0.5 nm, respectively.

HPLC with column oven and gradient pump (Lab Alliance), degasser (Systec) 20 μL injection loop (Rheodyn), interface (Pikokrom: Dizge Analitik), fluorescence dedector (FD) (Schimadzu) were used for the measurement of harmane concentration. Macherey Nagel Nucleosil 120-5 C18 column was used for the chromatographic separation of harmane. Emission and excition wavelengths of FD were adjusted to 300 and 435 nm, respectively. A mixture of KH_2PO_4/K_2HPO_4 (17.5 mmol/L)-methanol (30:70, v/v) was used as a mobile phase at a flow rate of 1.0 mL/min [33].

2.3. Synthesis of cMWCNT-γ-Fe_2O_3 magnetic nanoparticle

MWCNT as purchased was subjected to strong acidic conditions to open the side and end wall of the tube for carboxylating [36]. For this purpose, 1.25 g of MWCNT was refluxed in 50 mL of 1.0 mol/L HNO_3 for a day. Then, it was dispersed in a mixture of H_2SO_4 and HNO_3 (3:1, v/v) and sonicated at 30 °C for 5.0 h. Then, cMWCNT (oxidized and shortened) was filtered and dried at oven at 85 °C for a day. $FeCl_3 \cdot 6H_2O$ and $FeCl_2$ (mole ratio 2:1) were dissolved in 40 mL of distilled water and 0.1 g of cMWCNT was added to it by vigorously stirring. 30 mL of NH_3 was added dropwise for a time of 60 min at 80 °C. Resulting black solution was filtered and cMWCNT-γ-Fe_2O_3 as black precipitate was washed with distilled water untill it was neutral. Then, it was dried in oven at 90 °C for a day.

2.4. Characterization of cMWCNT-γ-Fe_2O_3 magnetic nanoparticle

Approximately 0.01 g of cMWCNT-γ-Fe_2O_3 and cMWCNT were weighted and inserted in a beaker. 3.0 mL of concentrated HCl and following mixture of 1.0 mL of $HN0_3$ and 0.5 mL of H_2O_2 were added to it and heated until dryness. Residues were dissolved in 50 and 5.0 mL of 1.0 mol/L $HN0_3$, respectively for cMWCNT-γ-Fe_2O_3 MNPs and cMWCNT. Concentrations of Fe in cMWCNT-γ-Fe_2O_3 magnetic nanoparticle and cMWCNT functionalized from pristine MWCNT were determined by ICP-OES. Surface functionalities were investigated by comparing their FT-IR spectra. The spectra were recorded in the transmission mode. Chemical structure of γ-Fe_2O_3 nanoparticle functionalized with cMWCNT was determined by XRD. XRD traces were recorded from 2θ of 2–80° with a 0.02° step size. VSM was employed to determine the magnetic saturation value of cMWCNT-γ-Fe_2O_3 magnetic nanoparticles at room temperature. SEM was used for characterization of macrostructure of materials with different resolutions. The morphology and microstructure of cMWCNT-γ-Fe_2O_3 magnetic nanoparticles were investigated by HR-TEM.

2.5. Antimicrobial activity studies

The antimicrobial activities of γ-Fe_2O_3, cMWCNT, and cMWCNT-γ-Fe_2O_3 were tested by agar-well diffusion methods. Bacterial strains were cultured overnight in Nutrient Broth (NB) at 37 °C with the exception of *C. albicans* cultured at 30 °C. A suspension of the tested microorganism (0.1 mL of 10^8 cells per mL) was spread on the Nutrient Agar (NA) plates. Wells of 6-mm diameter were filled with 0.1 mL of suspensions (1.5, 5.0 and 10 mg/mL). Plates were incubated at 37 °C for 24 h for bacteria and at 30 °C for 48 h for the yeast. 0.9% NaCl used as a control. The diameters of the inhibitory zones were measured in millimeters.

All the tests were performed in triplicate.

2.6. Adsorption of harmane of cMWCNT-γ-Fe_2O_3

Adsorption of harmane on cMWCNT-γ-Fe_2O_3 was investigated on batch conditions. For this purpose, acidity of 100 mL of 10.0 mg/L of aqueous harmane solution was adjusted to pH 7.0 and then 20 mg of cMWCNT-γ-Fe_2O_3 was added. It was magnetically stirred for 30 min at 100 rpm. Temperature was kept at 25 °C in preliminary experiments. Ionic strength of solution was adjusted to 0.1 mol/L using NaCl. Harmane adsorbed on magnetic nanoparticles was removed magnetically and released with methanol and its concentration was determined by HPLC with fluorescence detector. The amount of adsorbed harmane was calculated from the equation given in literatures [37,38]. Effects of pH, amount of nanoparticle, initial harmane concentrations and ionic strength on adsorption procedure were investigated in the ranges of pH 3.0-8.0, 0.5-75.0 mg/L of harmane and 0.1-1.0 mol/L of NaCl, respectively. Phosphate buffer, methanol, ethanol, acetonitrile, acetate buffer were examined for the release of harmane. Langmuir and Freundlich isotherms were employed to explain the adsorption of harmane on cMWCNT-γ-Fe_2O_3.

3. Results and discussions

3.1. Characterization of cMWCNT-γ-Fe_2O_3

Surface functionalities of synthesized magnetic nanoparticle were investigated by considering the spectroscopic results from FT-IR studies. Overlay spectra were presented in Fig. 1. The broad band at approximately 3400–3500 cm^{-1} showed the presence of surface hydroxyls of γ-Fe_2O_3 in Fig. 1a. The peaks at 632 and 585 cm^{-1} were characteristic peaks for Fe–O vibrations of γ-Fe_2O_3. Peak at nearly 1500 cm^{-1} was attributed to carboxyl groups of cMWCNT in Fig. 1b. From Fig. 1c –OH peaks from γ-Fe_2O_3 was not monitored due to binding to carboxyl groups in cMWCNT. Strong peak at 1550 cm^{-1} was attributed to formation of ester groups from c-MWCNT and γ-Fe_2O_3. A weak band in 1700 cm^{-1} region was correspond to C=O of acid or ester.

Structure of MNPs was determined from XRD experiments. XRD patterns of hybride structure composed from SPIONs and carboxyl modified MWCNT were given in Fig. 2. From the XRD peaks, exact structure of SPIONs was determined as γ-Fe_2O_3 and compared with those of reported in literature [39] and spectral library of instrument (Maghemite-Q, Card No. 25-1402). A series of characteristic peaks at 2θ=30.5°, 35.8°, 43.8°, 54.2°, 57.7°, and 63.2°, which correspond to (220), (311), (400), (422), (511), and (440) Bragg reflection, respectively, in Fig. 2. agreed with standard maghemite (γ-Fe_2O_3) XRD patterns [40]. From the Fig. 2 the diffraction peak at 2θ=26° ascribed to the (002) reflection of the MWCNT was confirmed the bonding of MWCNT to SPIONs [25,41]. Peaks with reflections 100 and 101 were not assigned due to low signal to noise ratio.

Fe concentrations in pristine MWCNT and cMWCNT-γ-Fe_2O_3 were measured by ICP-OES. Prior to instrumental detection, concentrated HCl and following mixture of $HN0_3$ and H_2O_2 (1:1, v/v) were added to samples on hot plate. Fe concentration in pristine MWCNT was found as 13,240 mg/kg while it was found as 31.1% in cMWCNT-γ-Fe_2O_3 MNPs. While Fe amount in pure γ-Fe_2O_3 was considered as 70%, it could be concluded MWCNT was reacted with γ-Fe_2O_3 to give a new product of γ-Fe_2O_3 coated with MWCNT.

It is known form the literature that MNPs should have superparamagnetic behavior at room temperature for targeted biomedical applications [11]. Magnetic properties of the cMWCNT-γ-Fe_2O_3

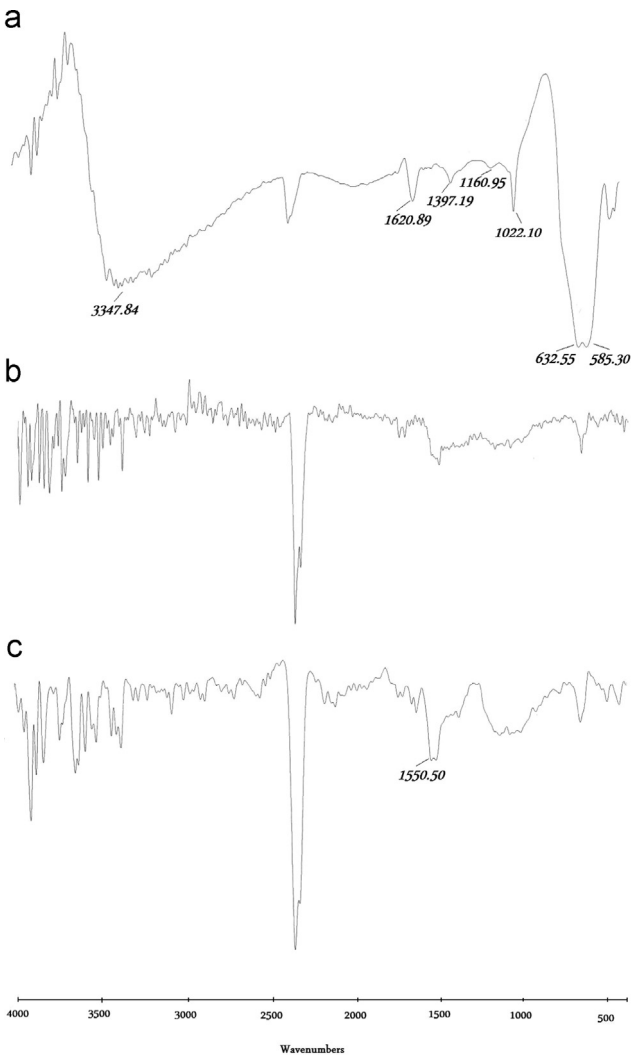

Fig. 1. Comparison of FT-IR spectra of (a) γ-Fe_2O_3 magnetic nanoparticle, (b) MWCNT, (c) MWCNT conjugted with γ-Fe_2O_3 magnetic nanoparticle.

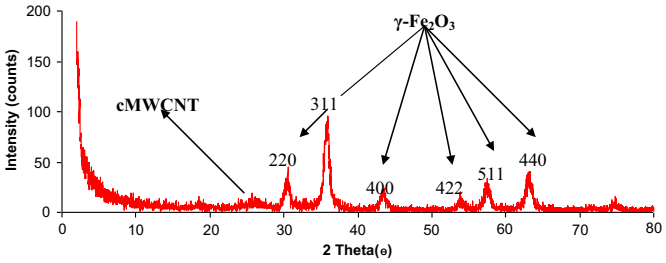

Fig. 2. XRD pattern of MWCNT-γ-Fe_2O_3 magnetic nanoparticle.

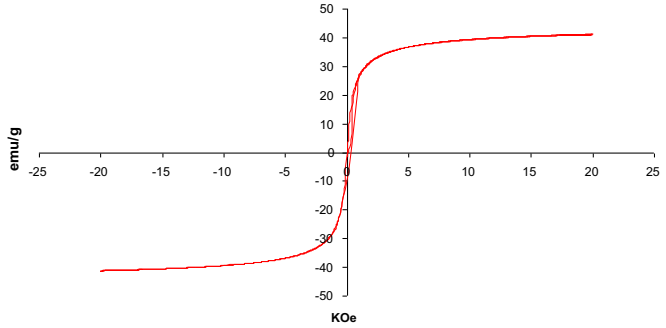

Fig. 3. VSM magnetization curve of MWCNT-γ-Fe_2O_3 magnetic nanoparticle.

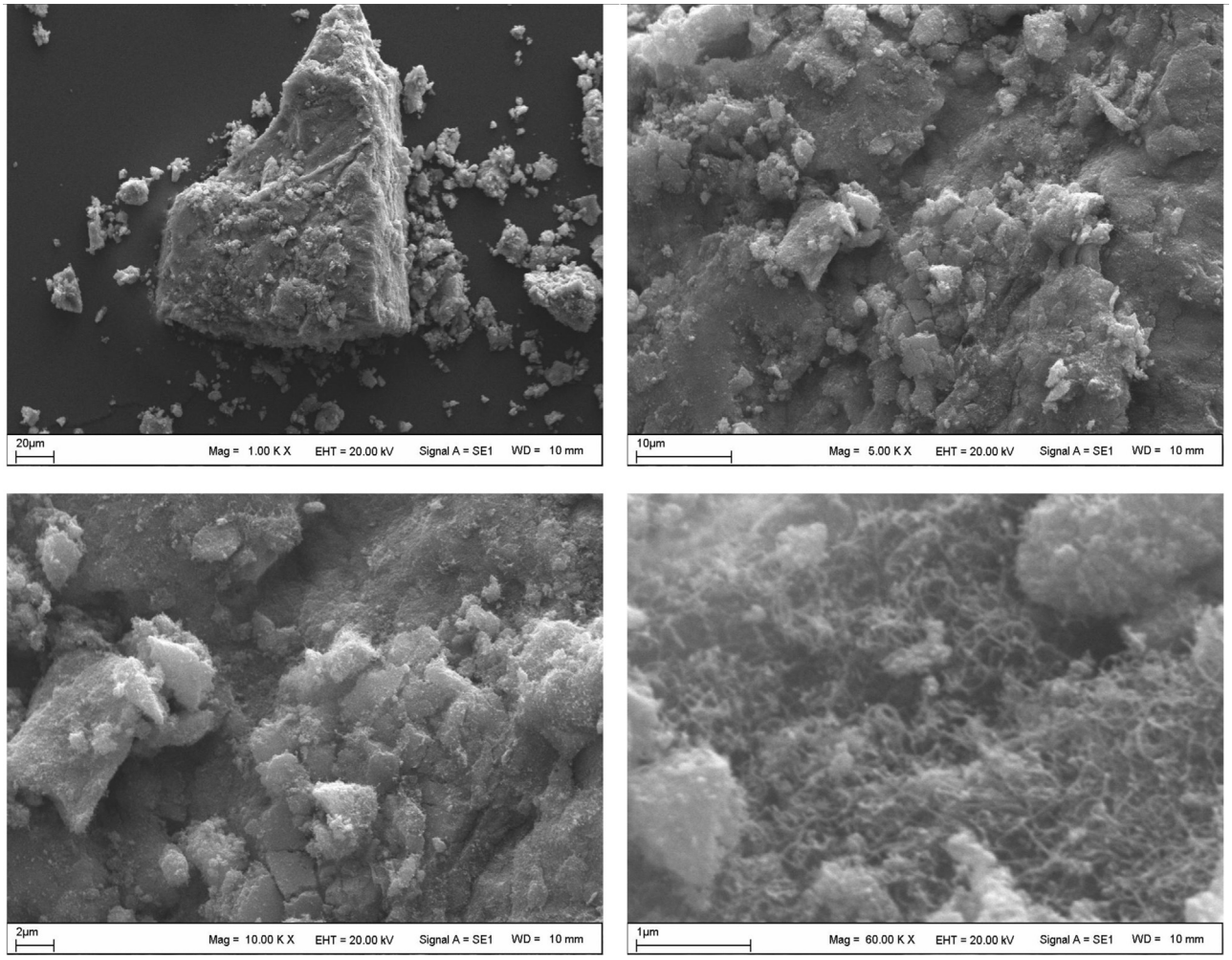

Fig. 4. Comparison of SEM images of MWCNT-γ-Fe_2O_3 magnetic nanoparticle.

were investigated by VSM analysis. Magnetization curve of the cMWCNT-γ-Fe_2O_3 MNPs was shown in Fig. 3. These particles exhibited superparamagnetic characteristics. Magnetization saturation was found as as 35.2 emu/g. From the results it could be said that cMWCNT-γ-Fe_2O_3 could be easily and reliably targeted through the specific applications.

SEM and HR-TEM were employed to investigate the microstructure and morphology of cMWCNT-γ-Fe_2O_3 MNPs. SEM images were presented in Fig. 4. with different resolutions as 20, 10, 2 and 1 μm showed the uniform size distribution. Agglomeration was observed from SEM images that attributed to the large free surface energy of each nanoparticle as well as their hydrophilicity [42]. Size of nanoparticle and arrangemement of its on cMWCNT were not possible to discuss due to low resolution and low particle size of MWCNT and SPIONs. From this point of view HR-TEM was employed to give more detailed surface information. HR-TEM images of cMWCNT-γ-Fe_2O_3 magnetic nanoparticles at different resolutions were given in Fig. 5. The main nearly spherical structure of MNPs was clearly seen. It was observed from HR-TEM images that the agglomeration of γ-Fe_2O_3 was protected by deposition of MNPs. It could also be concluded that cMWCNT was in core structure coated with γ-Fe_2O_3 as shell. It was also possible to discuss that functionalization of MWCNT through the carboxyl modification was occured in sidewalls of MWCNT. Additionally, spherical particles with size lower than 5 nm arranged on cMWCNT were also clear to see. For *in vivo* applications the magnetic particles must be coated with a biocompatible shell to prevent the formation of large aggregates.

3.2. Antimicrobial activity studies

Antimicrobial activities of γ-Fe_2O_3, cMWCNT, and cMWCNT-γ-Fe_2O_3 against microorganisms were examined in the present study and their potency was assessed by the presence or absence of inhibition zones and zone diameter. However no antimicrobial activity against tested microorganisms was observed (data not shown).

3.3. Adsorption and release of harmane

pH is one of the most important parameters which effects the adsorption and release behaviors of related analyte [38]. Effect of pH on adsorption of harmane was investigated in the ranges of pH 4.0–8.0. pH of the solutions were adjusted by adding required amounts of NaOH and HNO_3. Initial harmane concentration was selected as 10.0 mg/L. Maximum adsorption capacity of cMWCNT-γ-Fe_2O_3 was found as 23.4 mg/g for pH 4.0, 26.5 mg/g for pH 5.0, 32.3 mg/g for pH 6.0, 38.6 mg/g for pH 7.0, 34.4 mg/g for pH 8.0. Thus, pH was adopted as 7.0 for further experiments.

Effect of inital harmane concentration on adsorption was investigated in the ranges of 0.5–75.0 mg/L of harmane. Results were presented in Fig. 6a. It could be concluded that the capacity of cMWCNT-γ-Fe_2O_3 increased up to approximately 50 mg/L. A plateau was observed in this region after surface saturation and

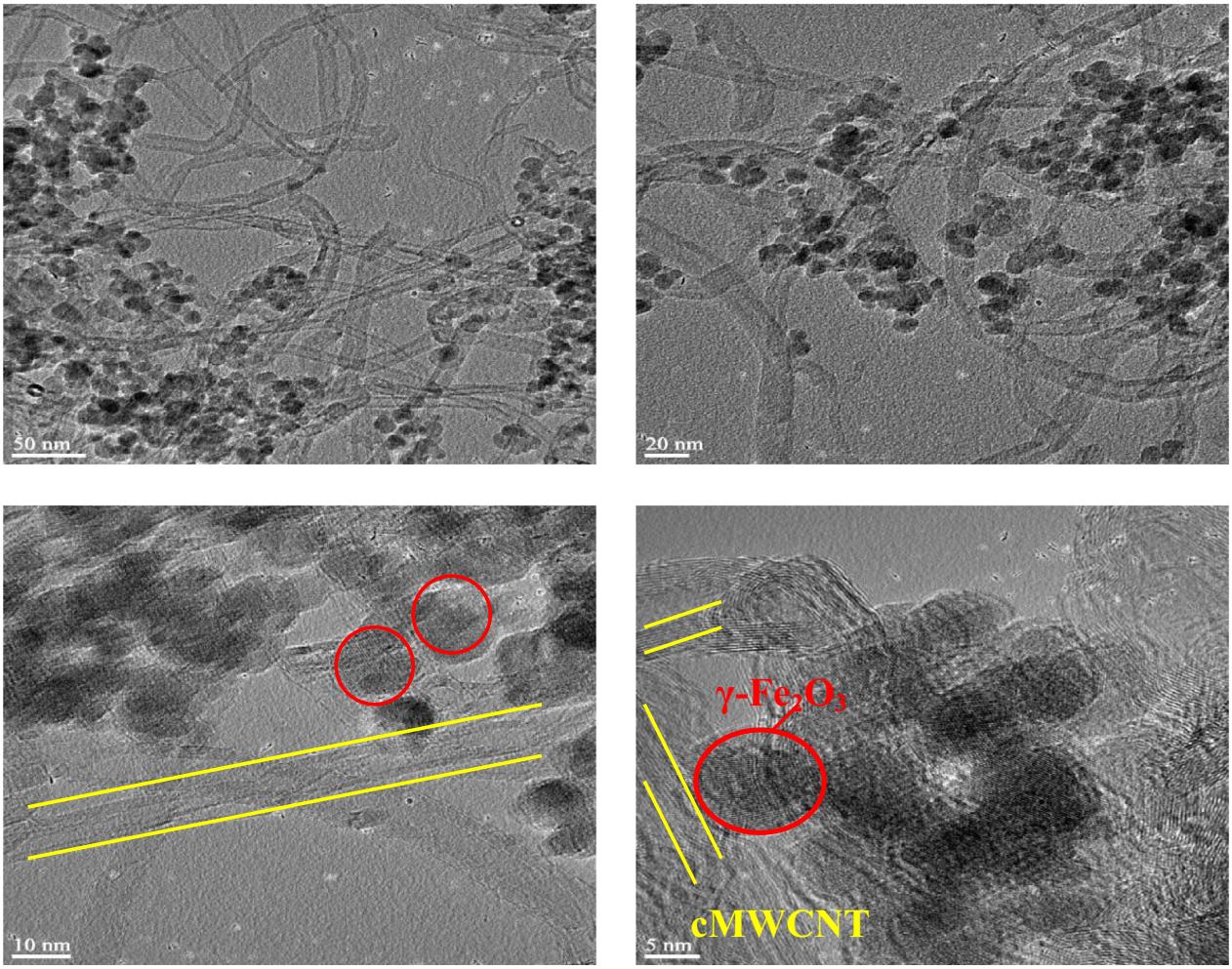

Fig. 5. Comparison of TEM and HR-TEM images of MWCNT-γ-Fe_2O_3 magnetic nanoparticle at different resolution (red line with respect to γ-Fe_2O_3 shell and yellow line with respect to cMWCNT). (For interpretation of the references to color in this figure legend, the reader is referred to the web version of this article.)

coating with harmane. Ionic strength of the solution was investigated in the ranges of 0.1–1.0 mol/L. As seen in Fig. 6b, decreasing was observed with increasing in ionic strength. Effect of amount of cMWCNT-γ-Fe_2O_3 on adsorption of harmane was investigated in the ranges of 5.0–50.0 mg and presented in Fig. 6c. Decreasing was observed with increasing in magnetic nanoparticle amount. It was attributed to interference between the binding sites at higher concentrations and possible agglomeration of magnetic nanoparticles. Higher specific adsorption of harmane at lower nanoparticle amounts could be due to an increased sorbent-to-adsorbent ratio, which decreases upon an increase in amount of nanoparticle.

Langmuir and Freundlich isotherms were applied to understand the adsorption mechanism [37]. Isotherm constants were summarized in Table 1. *As* is the maximum amount of the metal ions per unit weight of biosorbents to form a complete monolayer on the surface bound at high c_{eq} (equilibrium harmane concentration), and K_b is a constant related to the affinity of the binding sites. *As* represents a practical limiting adsorption capacity when the surface is fully covered with harmane and assists in the comparison of adsorption performance, particularly in cases where the sorbent did not reach its full saturation in experiments. The Langmuir equation is valid for monolayer sorption onto a homogeneous surface with a limited number of identical sites. The empirical Freundlich equation is based on a monolayer adsorption by the adsorbent with a heterogeneous energy distribution of active sites. K_F and n (it is desired to be $0.1 < n < 1$) are indicators of adsorption capacity and adsorption intensity, respectively. The Freundlich isotherm is also more widely used but provides no information on the monolayer adsorption capacity, in contrast to the Langmuir model. From Table 1, it could be concluded that adsoption of harmane on cMWCNT-γ-Fe_2O_3 well fitted to Langmuir equation with high correlation coefficient. 151.5 mg/g of maximum adsorption capacity was calculated from Langmuir equation. It could be discussed that magnetic nanoparticles had high surface area at nanometer scale. High affinity of magnetic nanoparticle to harmane was validated with K_b value as 255 mL/mg.

Adsorbed harmane on cMWCNT-γ-Fe_2O_3 was released with phosphate buffer, methanol, ethanol, acetonitrile, acetate buffer after magnetic decantation. For this purpose, 5.0 mL of each of reagents was added to it and concentrations of harmane in these were determined by HPLC with FD. Results were presented in Table 2. It was determined that methanol was an effective reagent for the release of harmane from cMWCNT-γ-Fe_2O_3. Lower release values were obtained when ethanol, acetonitrile, phosphate and acetate buffers were tried. Improving in release efficiency was achieved by adding of methanol to phosphate buffer that pH of its was adjusted to pH 7.0 by adding NaOH and HNO_3. 95.6% of harmane was released and determined by HPLC after magnetic separation. From this perspective, it could be concluded that cMWCNT-γ-Fe_2O_3 could be used for harmane targeted application include delivery, controlled release and detection.

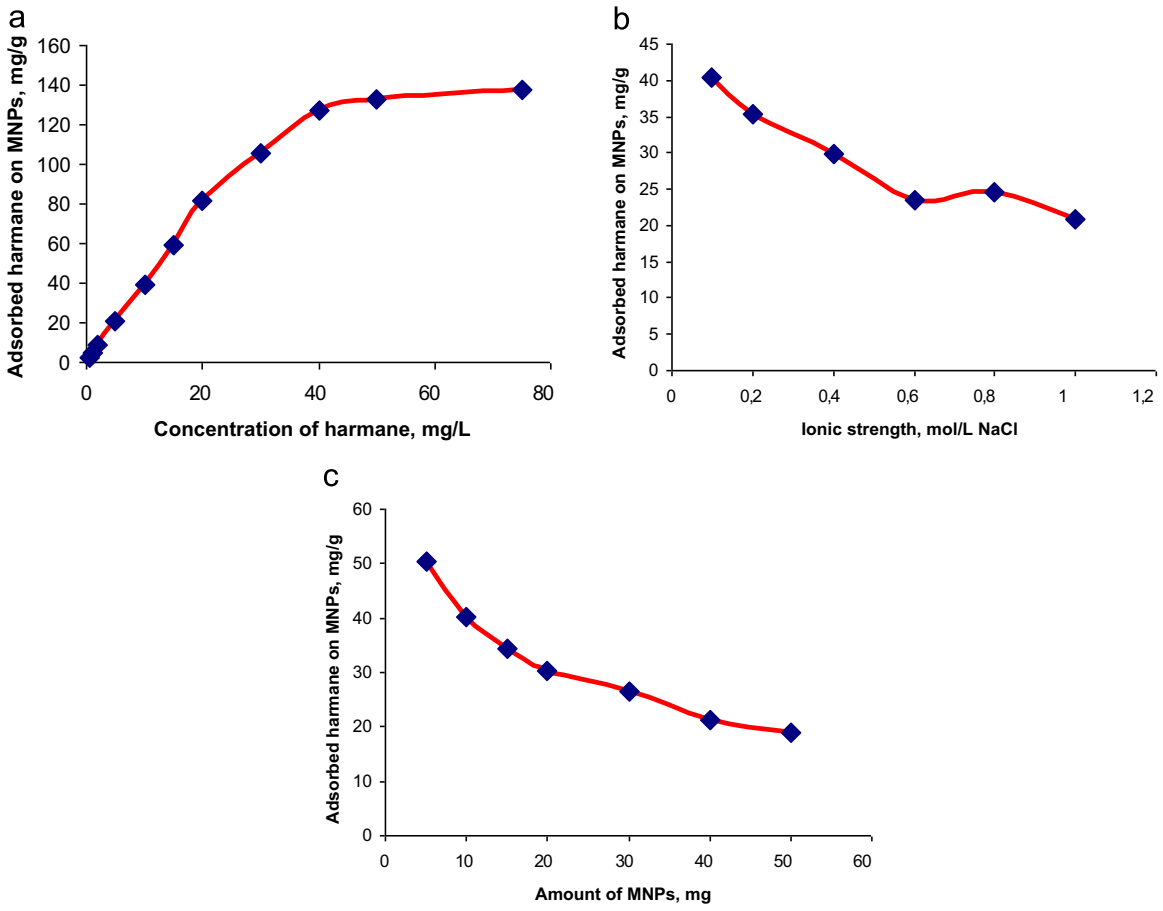

Fig. 6. (a). Effect of initial harmane concentration on adsorption to cMWCNT-γ-Fe_2O_3. Temperature 25 °C, ionic strength 0.1 mol/L of NaCl, pH 7.0, 20.0 mg of cMWCNT-γ-Fe_2O_3 (6b). Effect of ionic strength on adsorption of harmane to cMWCNT-γ-Fe_2O_3. Temperature 25 °C, harmane concentration 10.0 mg/L, pH 7.0, 20.0 mg of cMWCNT-γ-Fe_2O_3 (6c). Effect of amount of cMWCNT-γ-Fe_2O_3 on adsorption of harmane. Temperature 25 °C, harmane concentration 10.0 mg/L of 100.0 ml of harmane, pH 7.0.

Table 1
Langmuir and Freundlich iostherm constants for harmane adsorption on cMWCNT-γ-Fe_2O_3.

Langmuir isotherm		Freundlich isotherm	
A_s	151.5 mg/g	n	1.63
K_b	255 mL/mg	K_F	22.61
r^2	0.9924	r^2	0.9636

Table 2
Release of of harmane from cMWCNT-γ-Fe_2O_3, temperature 25 °C, 10.0 mg/L of 100.0 ml of harmane, pH 7.0, 20.0 mg of cMWCNT-γ-Fe_2O_3.

Release reagent	Releasing recovery (%)
Methanol	94.5
Ethanol	86.2
Acetonitrile	56.5
Acetate buffer, pH 7.0	75.5
Phosphate buffer, pH 7.0	82.2
Phosphate buffer, pH 7.0 contain 5% of methanol	95.6

4. Conclusion

A hybride nanoparticle composed of SPIONs and carboxyl functionalized MWCNT was synthesized and characterized by XRD, FT-IR, SEM, HRTEM, VSM, ICP-OES. Particle size of the product was lower than 10 nm that suitable for *in vivo* studies and targeted biomedical applications. From TEM and HR-TEM images, it was clear that SPIONs with spherical structure were arranged on the tube axis of the cMWCNT showed the side and end wall functionalization of MWCNT. Magnetic saturation value of cMWCNT-γ-Fe_2O_3 as 35.2 emu/g provided the magnetic separation by external magnetic field. Experiments on adsorption of harmane by cMWCNT-γ-Fe_2O_3 presented the high adsorption capacity of its through the spesific targeting. Phosphate buffer at pH 7.0 contain 5% of methanol was determined as release reagent with high release recovery. Experimental data showed that monolayer adsorption of harmane was valid from Langmuir isotherm. As a consequence, cMWCNT-γ-Fe_2O_3 magnetic nanomaterials are expected to have wide applications in nanobiotechnology and nanomedicine.

Acknowledgment

The author is grateful to Assistant Prof. Dr. Nesrin Haşimi from Batman University to investigations the antimicrobial activity of C_{60}-γ-Fe_2O_3 MNPs and discussions on results.

References

[1] R. Partha, L.R. Mitchell, J.L. Lyon, P.P. Joshi, J.L. Conyers, ACS Nano 2 (2008) 1950–1958.
[2] E. Kamalha, X. Shi, J.I. Mwasiagi, Y. Zeng, Macromol. Res. 20 (2012) 891–898.
[3] M.F. Frasco, N. Chaniotakis, Sensors 9 (2009) 7266–7286.
[4] J. Gao, H. Gu, B. Xu, Acc. Chem. Res. 42 (2009) 1097–1107.

[5] J. Dobson, Drug Dev. Res. 67 (2006) 55–60.
[6] R. Hao, R. Xing, Z. Xu, Y. Hou, S. Gao, S. Sun, Adv. Mater. 22 (2010) 2729–2742.
[7] L. Stanciu, Y. Won, M. Ganesana, S. Andreescu, Sensors 9 (2009) 2976–2999.
[8] C. Thammawong, P. Sreearunothai, A. Petchsuk, P. Tangboriboonrat, N. Pimpha, P. Opaprakasit, J. Nanopart. Res. 14 (2012) 1046–1053.
[9] C.G.C.M. Netto, H.E. Toma, L.H. Andrade, J. Mol. Catal. B: Enzym. 85–86 (2013) 71–92.
[10] Y. Ye, B. Geng, CRC Crit. Rev. Sol. State 37 (2012) 75–93.
[11] P. Tartaj, M.P. Morales, S. Veintemillas-Verdaguer, T. Gonzalez-Carreno, C. J. Serna, J. Phys. D Appl. Phys. 36 (2003) 182–197.
[12] M.V. Yiğit, A. Moore, Z. Medarova, Pharm. Res. 29 (2012) 1180–1188.
[13] S.P. Gubin, Y.A. Koksharov, G.B. Khomutov, G.Y. Yurkov, Russ. Chem. Rev. 74 (2005) 489–520.
[14] B. Zhang, H. Zhang, X. Li, X. Lei, C. Li, D. Yin, X. Fan, Q. Zhang, Mater. Sci. Eng. C 33 (2013) 4401–4408.
[15] H. Shokrollahi, Mater. Sci. Eng. C 33 (2013) 2476–2487.
[16] H.H.P. Yiu, M.A. Keane, J. Chem. Technol. Biotechnol. 87 (2012) 583–594.
[17] Z. Xu, Y. Hou, S. Sun, J. Am. Chem. Soc. 129 (2007) 8698–8699.
[18] F.M. Kievit, M. Zhang, Acc. Chem. Res. 44 (2011) 853–862.
[19] A. Lu, E.L. Salabas, F. Schüth, Angew. Chem. Int. Ed. 46 (2007) 1222–1244.
[20] S. Iijima, Nature 354 (1991) 56–58.
[21] M. Prato, K. Kostarelos, A. Bianco, Acc. Chem. Res. 41 (2008) 60–68.
[22] S. Ji, C. Liu, B. Zhang, F. Yang, J. Xu, J. Long, C. Jin, D. Fu, Q. Ni, X. Yu, Biochim. Biophys. Acta 1806 (2010) 29–35.
[23] M. Foldvari, M. Bagonluri, Nanomed.: Nanotechnol. 4 (2008) 173–182.
[24] D. Yang, F. Yang, J. Hu, J. Long, C. Wang, D. Fu, Q. Ni, Chem. Commun. 29 (2009) 4447–4449.
[25] Y. Shan, K. Chen, X. Yu, L. Gao, Appl. Surf. Sci. 257 (2010) 362–366.
[26] D. Xiao, P. Dramou, H. He, L.A. Pham-Huy, H. Li, Y. Yao, C. Pham-Huy, J. Nanopart. Res. 14 (2012) 984–1005.
[27] H. Zhang, Y. Shi, Anal. Chim. Acta 724 (2012) 54–60.
[28] H. Song, H. Liu, X. Jin, C. Min, J. Nanopart. Res. 14 (2012) 1290–1297.
[29] J. Ding, Q. Gao, X. Li, W. Huang, Z. Shi, Y. Feng, J. Sep. Sci. 34 (2011) 2498–2504.
[30] J. Marroquin, H.J. Kim, D. Jung, K.Y. Rhee, Carbon Lett. 13 (2012) 126–129.
[31] J. Deng, X. Wen, Q. Wang, Mater. Res. Bull. 47 (2012) 3369–3376.
[32] E.D. Louis, W. Jiang, K.M. Pellegrino, E. Rios, P. Factor-Litvak, C. Henchcliffe, W. Zheng, Neurotoxicology 29 (2008) 294–300.
[33] W. Zheng, S. Wang, L.F. Barnes, Y. Guan, E.D. Louis, Anal. Biochem. 279 (2000) 125–129.
[34] L. Agui, C. Pena-Farfal, P. Yanez-Sedeno, J.M. Pingarron, Anal. Chim. Acta 585 (2007) 323–330.
[35] E. Kılınc, F. Aydın, Anal. Lett. 45 (2012) 2623–2636.
[36] K.V. Singh, R.R. Pandey, X. Wang, R. Lake, C.S. Ozkan, K. Wang, M. Ozkan, Carbon 44 (2006) 1730–1739.
[37] S. Özdemir, E. Kilinc, A. Poli, B. Nicolaus, K. Güven, Chem. Eng. J. 152 (2009) 195–206.
[38] S. Ozdemir, F.M. Bekler, V. Okumus, A. Dundar, E. Kilinc, Environ. Prog. Sustain. Energy 31 (2012) 544–552.
[39] S.K. Sahoo, K. Agarwal, A.K. Singh, B.G. Polke, K.C. Raha, Int. J. Eng. Sci. Technol. l2 (2010) 118–126.
[40] N.G. Sahoo, H. Bao, Y. Pan, M. Pal, M. Kakran, H.K.F. Cheng, L. Li, L.P. Tan, Chem. Commun. 47 (2011) 5235–5237.
[41] Q. Zhang, M. Zhu, Q. Zhang, Y. Li, H. Wang, Compos. Sci. Technol. 69 (2009) 633–638.
[42] X. Liu, M.D. Kaminski, Y. Guan, H. Chen, H. Liu, A.J. Rosengart, J. Magn. Magn. Mater. 306 (2006) 248–253.